Contrib. Astron. Obs. Skalnaté Pleso **50**, 128 – 138, (2020)
https://doi.org/10.31577/caosp.2020.50.1.128

On the semiclassical perturbation Stark shifts of Ar II spectral lines

R. Hamdi[1,2], **N. Ben Nessib**[3], **S. Sahal-Bréchot**[4] **and M.S. Dimitrijević**[5,4]

[1] *Deanship of Joint First Year, Department of Physics, Umm Al-Qura University, Makkah, Saudi Arabia.*

[2] *Groupe de Recherche en Physique Atomique et Astrophysique, Faculté des Sciences de Bizerte, Université de Carthage, Tunisia., (E-mail: rafik.hamdi@istls.rnu.tn)*

[3] *Department of Physics and Astronomy, College of Science, King Saud University. PO Box 2455, Riyadh 11451, Saudi Arabia.*

[4] *Sorbonne Université, Observatoire de Paris, Université PSL, CNRS, LERMA, F-92190, Meudon, France*

[5] *Astronomical Observatory, Volgina 7, 11060 Belgrade, Serbia.*

Received: August 5, 2019; Accepted: September 28, 2019

Abstract. We present in this paper Stark shifts as a function of temperature for 20 spectral lines of Ar II belonging to 4p - 4d transition array. Calculations are made using semiclassical perturbation approach in impact approximation. Atomic data used in this calculation are carried out using Hartree-Fock method with relativistic corrections. Singly charged argon (Ar II) spectral lines are observed in many astrophysical plasmas. Ar II spectral lines are also important for laboratory plasmas and laser physics and technology.

Key words: atomic data – atomic processes – line: formation

1. Introduction

Inert gas such as argon produces very favorable conditions for stable discharges. For this reason argon plasmas are very attractive for testing the methods of plasma spectroscopy (Wiese, 1988). Singly charged argon (Ar II) spectral lines have been widely observed and studied in laboratory plasma. For example, Belmonte et al. (2014) measured transition probabilities for same UV lines of Ar II. Djurović et al. (2013) reported Stark broadening parameters measurements of Ar II UV lines. Gajo et al. (2013) measured Stark widths and shifts of Ar II spectral lines in the visible part of the spectrum. Ar II spectral lines are also used in plasma diagnostic. Alonso-Medina & Colón (2007) used Ar II spectral lines for the determination of temperature and electron density of laser induced lead plasma. Beside laboratory plasmas, singly charged argon spectral lines are also of interest for argon laser (Dimitrijević & Csillag, 2006). Ar II spectral lines

are also observed in stellar atmospheres. Vennes et al. (2018) performed abundance analysis of hot subdwarfs, they found a remarkable excess of argon with respect to oxygen in the hot subdwarf J2205-3141. Based on high resolution, high signal to noise observations of Ar II absorption lines, Brown et al. (1992) obtained abundances of argon in main-sequence B-type stars.

Stark broadening parameters are of interest for a number of applications such as laser physics, laser produced plasmas, modelling and investigation of stellar atmospheres in particular determination of chemical abundance. Stark broadening data are also useful for laboratory plasmas diagnostic. Corfdir et al. (2019) used Stark shift as a temperature diagnostic of Cu dominated plasma.

In this paper, we present Stark shifts for twenty Ar II spectral lines belonging to 4p - 4d transition array. Our Stark shift are given as a function of temperature for collisions with electrons, protons singly charged helium and singly charged argon. Our calculation are carried out using semiclassical perturbation approach (Sahal-Bréchot, 1969a,b) (SCP). SCP method need a set of atomic data sufficiently compleat. In this work the needed set of atomic data is calculated using Hartree-Fock method with relativistic corrections (Cowan, 1981).

2. The method

Our Stark shifts are calculated using semiclassical perturbation approach. A detailed description of this formalism with all the innovations is given in Sahal-Bréchot (1969a,b, 1974, 1991); Fleurier et al. (1977); Dimitrijević et al. (1991); Dimitrijević & Sahal-Bréchot (1996); Sahal-Bréchot et al. (2014) and earlier papers.

The shift (d) (in angular frequency units) of an electron-impact shifted spectral line can be expressed as:

$$d \;=\; N \int v f(v) dv \int_{R_3}^{R_D} 2\pi\rho d\rho \sin(2\varphi_p) \tag{1}$$

where N is the electron density, $f(v)$ the Maxwellian velocity distribution function for electrons, ρ denotes the impact parameter of the incoming electron.

The phase shift φ_p due to the polarization potential (r^{-4}), is given in Section 3 of Chapter 2 in Sahal-Bréchot (1969a) and R_D is the Debye radius. The cut-off R_3 is described in Section 1 of Chapter 3 in Sahal-Bréchot (1969a).

SCP calculation of Stark shift need a relatively large number of atomic data comparing to modified semi-emperical method (Dimitrijević & Konjević, 1980). In this work, atomic data needed for SCP calculation are determined using Hartree-Fock method with relativistic corrections (Cowan, 1981). We use as for the width calculations an atomic model including 24 configurations: $3s^2\ 3p^5$; $3s^2\ 3p^4\ nl$ (nl = 4p, 4f, 5p, 5f, 6p, 6f, 6h, 7p, 7f, 7h) (odd parity) and $3s\ 3p^6$; $3s^2\ 3p^4\ n'l'$ ($n'l'$ = 3d, 4s, 4d, 5s, 5d, 5g, 6s, 6d, 6g, 7s, 7d, 7g) (even parity). We use

an *ab initio* procedure. In Tab. 1, we compare our wavelengths and oscillator strengths with the values taken from NIST database (Kramida et al., 2018). We can see from Tab. 1 that our wavelengths and oscillator strengths are in good agreement with NIST values. Only electric dipole transitions (E1) are taken into account in our calculations. We have checked that the use of magnetic dipole (M1) and electric quadrupole (E2) transitions have no influence on the results.

3. Results and discussion

Table 1. Our calculated wavelengths and oscillator strengths compared with the values taken from NIST database (Kramida et al., 2018).

Lower level (i)	Upper level (j)	λ (Å) This work	λ (Å) NIST	f_{ij} This work	f_{ij} NIST
(^3P) 4p $^4P^o_{3/2}$	(^3P) 4d $^4D_{5/2}$	3465.74	3514.39	0.377	0.378
(^3P) 4p $^4P^o_{1/2}$	(^3P) 4d $^4D_{3/2}$	3484.51	3535.32	0.265	0.21
(^3P) 4p $^4P^o_{5/2}$	(^3P) 4d $^4D_{5/2}$	3428.10	3467.75	0.220	0.227
(^3P) 4p $^4P^o_{1/2}$	(^3P) 4d $^4D_{1/2}$	3463.75	3509.78	0.373	0.471
(^3P) 4p $^4P^o_{5/2}$	(^3P) 4d $^4D_{3/2}$	3406.92	3454.09	0.0385	0.0375
(^3P) 4p $^4P^o_{5/2}$	(^3P) 4d $^4P_{5/2}$	3108.72	3139.02	0.0796	0.077
(^3P) 4p $^4P^o_{3/2}$	(^3P) 4d $^4P_{3/2}$	3180.37	3212.52	0.0108	0.0081
(^3P) 4p $^4P^o_{1/2}$	(^3P) 4d $^4P_{1/2}$	3251.51	3281.71	0.0730	0.068
(^3P) 4p $^4P^o_{5/2}$	(^3P) 4d $^4P_{3/2}$	3148.64	3181.04	0.0454	0.037
(^3P) 4p $^4P^o_{3/2}$	(^3P) 4d $^4P_{1/2}$	3216.28	3243.69	0.0888	0.0833
(^3P) 4p $^4P^o_{3/2}$	(^3P) 4d $^4P_{5/2}$	3139.64	3169.67	0.104	0.11
(^3P) 4p $^4P^o_{5/2}$	(^3P) 4d $^2F_{7/2}$	3091.66	3146.42	0.000438	0.00059
(^3P) 4p $^4D^o_{3/2}$	(^3P) 4d $^4D_{3/2}$	3772.17	3872.17	0.0367	0.034
(^3P) 4p $^4D^o_{7/2}$	(^3P) 4d $^4D_{7/2}$	3686.67	3780.84	0.184	0.17
(^3P) 4p $^4D^o_{5/2}$	(^3P) 4d $^4D_{5/2}$	3734.16	3826.81	0.0693	0.0617
(^3P) 4p $^4D^o_{1/2}$	(^3P) 4d $^4D_{1/2}$	3782.32	3880.33	0.0453	0.0524
(^3P) 4p $^4D^o_{7/2}$	(^3P) 4d $^4D_{5/2}$	3670.06	3763.50	0.0328	0.0284
(^3P) 4p $^4D^o_{5/2}$	(^3P) 4d $^4D_{7/2}$	3751.35	3844.73	0.014	0.0137
(^3P) 4p $^4D^o_{3/2}$	(^3P) 4d $^4D_{5/2}$	3798.15	3900.36	0.0295	0.025
(^3P) 4p $^4D^o_{1/2}$	(^3P) 4d $^4D_{3/2}$	3807.09	3911.58	0.0432	0.035

Our calculated Stark shifts are presented in Tab. 2 (see appendix) for twenty spectral lines belonging to 4p-4d transition array for a perturber density of 10^{17} cm^{-3} and for a set of temperatures from 5 000 K to 60 000 K. Stark shifts are given for electron- proton- singly ionized helium and singly ionized argon impact broadening, in this way we take into account the most important perturbers in stellar atmospheres and laboratory plasmas as well as for example for argon lasers. Since our results are obtained using calculated energy levels, a

correction to the shifts due to the difference between calculated and observed wavelengths is introduced using Eq. (8) of Hamdi et al. (2013). All wavelengths given in Tab. 2 are taken from NIST database (Kramida el al., 2018). The impact approximation is valid for all values given in Tab. 2 since the collision volume (V) multiplied by the pertureber density (N) is much less than one. When the impact approximation reaches its limit of validity ($0.1<N\,V\leq 0.5$), the value is preceded by an asterisk.

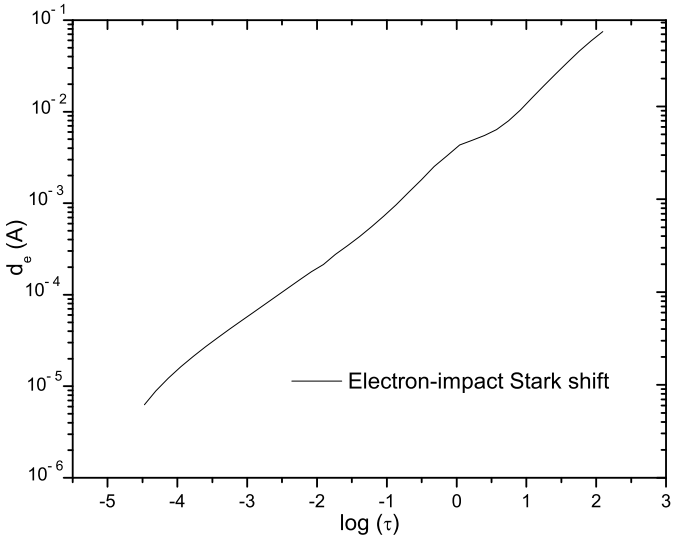

Figure 1. Electron-impact Stark shift for Ar II (^{3}P) 4p ^{4}P$^o_{3/2}$ - (^{3}P) 4d ^{4}D $_{5/2}$ (λ= 3514.39 Å) spectral line as a function of logarithm of Rosseland optical depth (log τ). Electron-impact Stark shift is shown for an atmospheric model (Kurucz, 1979) with surface gravity log g = 4.5 and effective temperature T$_{eff}$ = 10 000 K.

In Hamdi et al. (2019), we have compared our Stark shifts with experimental results (Djeniže et al., 1989; Dzierzega & Musiol, 1994; Aparicio et al., 1998; Djurović et al., 2013) for Ar II spectral lines. We found good agreement with experimental results except for some transitions. For example, the agreement with Djurović et al. (2013) was 27% for 4p-4d transitions except for four transitions. Concerning Stark widths, the comparison with experiments is made in Hamdi et al. (2017, 2018) for 212 spectral lines and we found an agreement generally good. For example, the average agreement for 4p-4d transitions was

10% comparing with Djurović et al. (2013) and 20% comparing with Pellerin et al. (1997).

In Fig. 1, we present the electron-impact Stark shift for Ar II (^{3}P) 4p ^{4}P$^o_{3/2}$ - (^{3}P) 4d ^{4}D $_{5/2}$ (λ= 3514.39 Å) spectral line as a function of logarithm of Rosseland optical depth (log τ) for an A-type star. Electron-impact Stark shift is shown for an atmospheric model (Kurucz, 1979) with surface gravity log g = 4.5 and effective temperature T$_{eff}$ = 10 000 K. Fig. 1 shows that the value of the electron-impact Stark shift in the deeper atmospheric layer is about 0.1 Å. The theoretical resolving power of the high-resolution echelle spectrometer for the Keck TenMeter Telescope is of the order of > 250,000, but practical realizations may be approximately 36,000. For λ = 3514.39 Å, this resolving power enables to register shifts of 0.08 Å. Since new generations of terrestrial telescopes, as for example European Extremely Large Telescope of 39.3 m will have even greater resolving power, shifts from deepest layers in Fig. 1 will be measurable with such telescopes in the near future.

4. Conclusion

We have presented Stark shifts for twenty 4p-4d spectral lines of Ar II ion calculated using semiclassical perturbation approach and a set of atomic data calculated using Hartree-Fock method with relativistic corrections. The accuracy of our method was checked in our previous work (Hamdi et al. 2019). The accuracy of the atomic data used as input parameters for SCP calculation of Stark shifts is also verified by comparing our wavelengths and our oscillator strengths with the values of NIST database. We hope that our results will be of interest for the investigation of laboratory and astrophysical plasmas.

Acknowledgements. This work is part of the project 176002 "Influence of collisional processes on astrophysical plasma line shapes" supported by the Ministry of Education, Science and Technological Development of Serbia. This work has been also supported by the Paris Observatory, the CNRS and the PNPS (Programme National de Physique Stellaire, INSU-CNRS), France. This work has also been supported by the LABEX Plas@par project, and received financial state aid managed by the Agence Nationale de la Recherche, as part of the programme "Investissements d'avenir" under the reference ANR--11--IDEX--0004--02.

References

Alonso-Medina, A. & Colón, C., Stark widths of several Pb III spectral lines in a laser-induced lead plasma. 2007, *Astron. Astrophys.*, **466**, 399, DOI: 10.1051/0004-6361:20066113

Aparicio, J.A., Gigosos, M.A., González, V.R., Pérez, C., de la Rosa, M.I., & Mar, S., Measurement of Stark broadening and shift of singly ionized Ar lines. 1998, *J. Phys. B*, **31**, 1029. DOI: 10.1088/0953-4075/31/5/011

Belmonte, M. T., Djurović, S., Peláez, R. J., Aparicio, J. A. & Mar, S., Improved and expanded measurements of transition probabilities in UV Ar II spectral lines. 2014, *Mon. Not. R. Astron. Soc.*, **445**, 3345, DOI: 10.1093/mnras/stu2006

Brown, P. J. F., Dufton, P. L., Keenan, F. P., Holmgren, D. E. & Warren, G. A., The determination of accurate cosmic abundances from B-type stellar spectra. 1992, in Lecture Notes in Physics, Vol. **401**, *The Atmospheres of Early-Type Stars*, ed. U. Heber & C.S. Jeffery, 33

Corfdir, P., Lantz, G., Abplanalp, M., Sütterlin, P., Kassubek, F., Delachaux, T. & Bator, M., Stark shift measurement as a temperature diagnostic of Cu-dominated thermal plasmas. 2019, *Journal of Physics D*, **52**, 5203, DOI: 10.1088/1361-6463/ab188e

Cowan, R. D. 1981, *The theory of atomic structure and spectra*

Dimitrijević, M. S. & Csillag, L., Influence of spectral line broadening on the mode structure of He-Kr and He-Ar gas lasers. 2006, *Journal of Applied Spectroscopy*, **73**, 458, DOI: 10.1007/s10812-006-0100-6

Dimitrijević, M. S. & Konjević, N., Stark widths of doubly- and triply-ionized atom lines. 1980, *J. Quant. Spectrosc. Radiat. Transf.*, **24**, 451, DOI: 10.1088/0031-8949/54/1/008

Dimitrijević, M. S. & Sahal-Bréchot, Stark broadening of neutral helium lines. 1984, *J. Quant. Spectrosc. Radiat. Transf.*, **31**, 301, DOI: 10.1016/0022-4073(84)90092-X

Dimitrijević, M. S. & Sahal-Bréchot, Stark broadening of Li II spectral lines. 1996, *Physica Scripta*, **54**, 50, DOI: 10.1088/0031-8949/54/1/008

Dimitrijević, M. S., Sahal-Bréchot, S. and Bommier, V., Stark broadening of spectral lines of multicharged ions of astrophysical interest. I - C IV lines. II - SI IV lines. 1991, *Astron. Astrophys., Suppl.*, **89**, 581,

Djeniže, S., Malešević, M., Srećković, A., Milosavljević, M. & Purić, P., Stark broadening and shift of singly-ionized argon spectral lines in higher multiplets. 1989, *J. Quant. Spectrosc. Radiat. Transf.*, **42**, 429, DOI: 10.1016/0022-4073(89)90011-3

Djurović, S., Belmonte, M. T., Peláez, R. J., Aparicio, J. A. & Mar, S., Stark parameter measurement of Ar II UV spectral lines. 2013, *Mon. Not. R. Astron. Soc.*, **433**, 1082, DOI: 10.1093/mnras/stt787

Fleurier, C., Sahal-Bréchot, S. & Chapelle, J., Stark profiles of some ion lines of alkaline earth elements. 1977, *J. Quant. Spectrosc. Radiat. Transf.*, **17**, 595, DOI: 10.1016/0022-4073(77)90019-X

Gajo, T., Mijatović, Z., Savić, I., Djurović, S. & Kobilarov, R., Stark widths and shifts of Ar II spectral lines in visible part of spectrum. 2013, *J. Quant. Spectrosc. Radiat. Transf.*, **127**, 119, DOI: 10.1016/j.jqsrt.2013.05.005

Dzierzega, K. & Musiol, K., Stark broadening and shift for Ar II lines. 1994, *J. Quant. Spectrosc. Radiat. Transf.*, **52**, 747. DOI: 10.1016/0022-4073(94)90040-X

Hamdi, R., Ben Nessib, N., Dimitrijević, M. S. & Sahal-Bréchot, S. , Stark broadening of Pb IV spectral lines. 2013, *Mon. Not. R. Astron. Soc.*, **431**, 1039, DOI: 10.1093/mnras/stt228

Hamdi, R., Ben Nessib, N., Sahal-Bréchot, S. & Dimitrijević, M. S., Stark Widths of Ar II Spectral Lines in the Atmospheres of Subdwarf B Stars. 2017, *Atoms*, **5**, 26, DOI: 10.3390/atoms5030026

Hamdi, R., Ben Nessib, N., Sahal-Bréchot, S. & Dimitrijević, M. S., Semiclassical perturbation Stark widths of singly charged argon spectral lines. 2018, *Mon. Not. R. Astron. Soc.*, **475**, 800, DOI: 10.1093/mnras/stx3209

Hamdi, R., Ben Nessib, N., Sahal-Bréchot, S. & Dimitrijević, M. S., Semiclassical perturbation Stark shifts of singly charged argon spectral lines. 2019, *Mon. Not. R. Astron. Soc.*, **488**, 2473, DOI: 10.1093/mnras/stz1835

Kramida, A., Ralchenko, Yu., Reader, J. & NIST ASD Team, 2018, NIST Atomic Spectra Database (ver. 5.6.1). National Institute of Standards and Technology, Gaithersburg, MD. Available at: https://physics.nist.g ov/asd. DOI: https://doi.org/10.18434/T4W30F

Kurucz, R. L., Model atmospheres for G, F, A, B, and O stars. 1979, *Astrophys. J., Suppl.*, **40**, 1, DOI: 10.1086/190589

Pellerin, S., Musiol, K., & Chapelle, J., Measurement of atomic parameters of singly ionized argon lines. III. Stark broadening parameters. 1997, *J. Quant. Spectrosc. Radiat. Transf.*, **57**, 377. DOI: 10.1016/S0022-4073(96)00134-3

Sahal-Bréchot, S., Impact Theory of the Broadening and Shift of Spectral Lines due to Electrons and Ions in a Plasma. 1969, *Astron. Astrophys.*, **1**, 91,

Sahal-Bréchot, S., Impact Theory of the Broadening and Shift of Spectral Lines due to Electrons and Ions in a Plasma (Continued). 1969, *Astron. Astrophys.*, **2**, 322,

Sahal-Bréchot, S., Stark Broadening of Isolated Lines in the Impact Approximation. 1974, *Astron. Astrophys.*, **35**, 319,

Sahal-Bréchot, S., Broadening of ionic isolated lines by interactions with positively charged perturbers in the quasistatic limit. 1991, *Astron. Astrophys.*, **245**, 322,

Sahal-Bréchot, S., Dimitrijević, M. S. & Ben Nessib, N., Widths and Shifts of Isolated Lines of Neutral and Ionized Atoms Perturbed by Collisions With Electrons and Ions: An Outline of the Semiclassical Perturbation (SCP) Method and of the Approximations Used for the Calculations. 2014, *Atoms*, **2**, 225, DOI: 10.3390/atoms2020225

Vennes, S., Németh, P. & Kawka, A., A FEROS Survey of Hot Subdwarf Stars. 2018, *Open Astronomy*, **27**, 7, DOI: 10.1515/astro-2018-0005

Wiese, W. L., The atomic transition probabilities of argon - a continuing challengeto plasma spectroscopy. 1988, *J. Quant. Spectrosc. Radiat. Transf.*, **40**, 421, DOI: 10.1016/0022-4073(88)90130-6

A. Stark shifts results

Table 2. Electron-, proton-, singly charged helium and singly-charged argon-impact Stark shifts for Ar II lines calculated using semiclassical perturbation approach (Sahal-Bréchot 1969a,b) and a set of atomic data is calculated using Cowan code (Cowan 1981), for a perturber density of 10^{17} cm^{-3} and temperatures of 5000 to 60 000 K. Wavelength of the transitions (in Å) and parameter C (Dimitrijević & Sahal-Bréchot 1984) are also given. This parameter when divided with the corresponding Stark width gives an estimate for the maximal pertuber density for which the line may be treated as isolated. d_e: electron-impact Stark shift, d_{H^+}: proton-impact Stark shift, d_{He^+}: singly charged helium-impact Stark shift, d_{Ar^+}: singly charged argon-impact Stark shift. Cells preceded by an asterisk mean that the impact approximation reaches its limit of validity ($0.1<NV\leq 0.5$). Empty cells mean that the impact approximation is not valid.

Transition	T (K)	d_e (Å)	d_{H^+} (Å)	d_{He^+} (Å)	d_{Ar^+} (Å)
(^3P) 4p $^4P^o_{3/2}$ - (^3P) 4d $^4D_{5/2}$	5000.	0.344	0.206E-01	*0.171E-01	
3514.39 A	10000.	0.265	0.321E-01	*0.259E-01	*0.185E-01
C= 0.56E+20	20000.	0.207	0.423E-01	0.347E-01	*0.253E-01
	30000.	0.184	0.478E-01	0.388E-01	*0.284E-01
	40000.	0.167	0.522E-01	0.431E-01	*0.314E-01
	60000.	0.147	0.580E-01	0.465E-01	*0.335E-01
(^3P) 4p $^4P^o_{1/2}$ - (^3P) 4d $^4D_{3/2}$	5000.	0.342	0.205E-01	*0.169E-01	
3535.32 A	10000.	0.261	0.319E-01	*0.257E-01	*0.191E-01
C= 0.54E+20	20000.	0.206	0.421E-01	0.346E-01	*0.263E-01
	30000.	0.183	0.473E-01	0.388E-01	*0.292E-01
	40000.	0.166	0.519E-01	0.426E-01	*0.324E-01
	60000.	0.146	0.577E-01	0.459E-01	*0.347E-01
(^3P) 4p $^4P^o_{5/2}$ - (^3P) 4d $^4D_{5/2}$	5000.	0.316	0.192E-01	*0.159E-01	
3476.75 A	10000.	0.241	0.301E-01	*0.243E-01	*0.181E-01
C= 0.55E+20	20000.	0.188	0.398E-01	0.325E-01	*0.248E-01
	30000.	0.169	0.447E-01	0.367E-01	*0.278E-01
	40000.	0.152	0.491E-01	0.400E-01	*0.307E-01

Table 2. continued

Transition	T (K)	d_e (Å)	d_{H^+} (Å)	d_{He^+} (Å)	d_{Ar^+} (Å)
(^{3}P) 4p $^4P^o_{1/2}$ - (^{3}P) 4d $^4D_{1/2}$	5000.	0.343	0.205E-01	*0.170E-01	
3509.78 A	10000.	0.264	0.320E-01	*0.258E-01	*0.192E-01
C= 0.55E+20	20000.	0.206	0.422E-01	0.346E-01	*0.265E-01
	30000.	0.184	0.477E-01	0.387E-01	*0.295E-01
	40000.	0.166	0.521E-01	0.429E-01	*0.326E-01
	60000.	0.147	0.578E-01	0.463E-01	*0.350E-01
(^{3}P) 4p $^4P^o_{5/2}$ - (^{3}P) 4d $^4D_{3/2}$	5000.	0.326	0.195E-01	*0.161E-01	
3454.09 A	10000.	0.250	0.304E-01	*0.246E-01	*0.183E-01
C= 0.52E+20	20000.	0.196	0.402E-01	0.330E-01	*0.252E-01
	30000.	0.176	0.452E-01	0.371E-01	*0.280E-01
	40000.	0.159	0.495E-01	0.407E-01	*0.310E-01
	60000.	0.140	0.551E-01	0.439E-01	*0.331E-01
(^{3}P) 4p $^4P^o_{5/2}$ - (^{3}P) 4d $^4P_{5/2}$	5000.	0.288	0.206E-01	*0.173E-01	
3139.02 A	10000.	0.222	0.322E-01	*0.254E-01	
C= 0.16E+20	20000.	0.174	0.425E-01	*0.347E-01	*0.264E-01
	30000.	0.154	0.475E-01	0.388E-01	*0.293E-01
	40000.	0.140	0.525E-01	0.430E-01	*0.323E-01
	60000.	0.122	0.573E-01	0.464E-01	*0.347E-01
	60000.	0.134	0.538E-01	0.431E-01	*0.328E-01
(^{3}P) 4p $^4P^o_{3/2}$ - (^{3}P) 4d $^4P_{3/2}$	5000.	0.308	0.217E-01	*0.183E-01	
3212.52 A	10000.	0.239	0.340E-01	*0.267E-01	
C= 0.21E+20	20000.	0.188	0.449E-01	*0.365E-01	*0.279E-01
	30000.	0.166	0.501E-01	0.408E-01	*0.308E-01
	40000.	0.151	0.555E-01	0.455E-01	*0.341E-01
	60000.	0.134	0.605E-01	0.490E-01	*0.365E-01
(^{3}P) 4p $^4P^o_{1/2}$ - (^{3}P) 4d $^4P_{1/2}$	5000.	0.348	0.245E-01	*0.205E-01	
3281.70 A	10000.	0.272	0.380E-01	*0.301E-01	
C= 0.28E+20	20000.	0.214	0.504E-01	*0.410E-01	*0.313E-01
	30000.	0.189	0.565E-01	0.458E-01	*0.349E-01
	40000.	0.173	0.625E-01	0.504E-01	*0.381E-01
	60000.	0.151	0.679E-01	0.544E-01	*0.417E-01
(^{3}P) 4p $^4P^o_{5/2}$ - (^{3}P) 4d $^4P_{3/2}$	5000.	0.302	0.212E-01	*0.180E-01	
3181.04 A	10000.	0.234	0.334E-01	*0.262E-01	
C= 0.20E+20	20000.	0.184	0.440E-01	*0.358E-01	*0.274E-01
	30000.	0.163	0.491E-01	0.400E-01	*0.302E-01
	40000.	0.148	0.544E-01	0.446E-01	*0.334E-01
	60000.	0.131	0.593E-01	0.480E-01	*0.357E-01

Table 2. continued

Transition	T (K)	d_e (Å)	d_{H^+} (Å)	d_{He^+} (Å)	d_{Ar^+} (Å)
(^{3}P) 4p $^4P^o_{3/2}$ - (^{3}P) 4d $^4P_{1/2}$	5000.	0.341	0.239E-01	*0.200E-01	
3243.69 A	10000.	0.265	0.371E-01	*0.294E-01	
C= 0.28E+20	20000.	0.210	0.492E-01	*0.401E-01	*0.305E-01
	30000.	0.185	0.552E-01	0.447E-01	*0.340E-01
	40000.	0.169	0.610E-01	0.492E-01	*0.372E-01
	60000.	0.148	0.663E-01	0.531E-01	*0.407E-01
(^{3}P) 4p $^4P^o_{1/2}$ - (^{3}P) 4d $^4P_{3/2}$	5000.	0.315	0.222E-01	*0.187E-01	
3249.80 A	10000.	0.244	0.349E-01	*0.274E-01	
C= 0.21E+20	20000.	0.191	0.459E-01	*0.374E-01	*0.285E-01
	30000.	0.170	0.513E-01	0.417E-01	*0.315E-01
	40000.	0.153	0.567E-01	0.465E-01	*0.349E-01
	60000.	0.136	0.619E-01	0.501E-01	*0.373E-01
(^{3}P) 4p $^4P^o_{3/2}$ - (^{3}P) 4d $^4P_{5/2}$	5000.	0.294	0.210E-01	*0.176E-01	
3169.67 A	10000.	0.226	0.329E-01	*0.259E-01	
C= 0.16E+20	20000.	0.177	0.435E-01	*0.354E-01	*0.269E-01
	30000.	0.157	0.485E-01	0.395E-01	*0.299E-01
	40000.	0.142	0.536E-01	0.439E-01	*0.329E-01
	60000.	0.125	0.585E-01	0.473E-01	*0.354E-01
(^{3}P) 4p $^4P^o_{5/2}$ - (^{3}P) 4d $^2F_{7/2}$	5000.	0.347	0.268E-01	*0.222E-01	
3146.42 A	10000.	0.271	0.406E-01	*0.323E-01	
C= 0.22E+20	20000.	0.215	0.544E-01	*0.441E-01	*0.340E-01
	30000.	0.189	0.604E-01	*0.497E-01	*0.376E-01
	40000.	0.173	0.675E-01	0.544E-01	*0.414E-01
	60000.	0.151	0.733E-01	0.583E-01	*0.444E-01
(^{3}P) 4p $^4D^o_{3/2}$ - (^{3}P) 4d $^4D_{3/2}$	5000.	0.404	0.245E-01	*0.202E-01	
3872.14 A	10000.	0.309	0.382E-01	*0.308E-01	*0.229E-01
C= 0.63E+20	20000.	0.240	0.504E-01	0.414E-01	*0.314E-01
	30000.	0.214	0.567E-01	0.466E-01	*0.349E-01
	40000.	0.194	0.620E-01	0.510E-01	*0.387E-01
	60000.	0.171	0.689E-01	0.549E-01	*0.413E-01
(^{3}P) 4p $^4D^o_{7/2}$ - (^{3}P) 4d $^4D_{7/2}$	5000.	0.376	0.231E-01	*0.191E-01	
3780.84 A	10000.	0.286	0.361E-01	*0.291E-01	*0.218E-01
C= 0.65E+20	20000.	0.221	0.478E-01	0.391E-01	*0.298E-01
	30000.	0.196	0.537E-01	0.441E-01	*0.330E-01
	40000.	0.177	0.586E-01	0.482E-01	*0.367E-01
	60000.	0.155	0.649E-01	0.520E-01	*0.391E-01

Table 2. continued

Transition	T (K)	d_e (Å)	d_{H^+} (Å)	d_{He^+} (Å)	d_{Ar^+} (Å)
(^3P) 4p $^4D^o_{5/2}$ - (^3P) 4d $^4D_{5/2}$	5000.	0.382	0.235E-01	*0.194E-01	
3826.81 A	10000.	0.290	0.366E-01	*0.296E-01	*0.221E-01
C= 0.65E+20	20000.	0.226	0.485E-01	0.397E-01	*0.302E-01
	30000.	0.201	0.545E-01	0.447E-01	*0.337E-01
	40000.	0.182	0.597E-01	0.487E-01	*0.373E-01
	60000.	0.159	0.657E-01	0.527E-01	*0.399E-01
(^3P) 4p $^4D^o_{1/2}$ - (^3P) 4d $^4D_{1/2}$	5000.	0.413	0.250E-01	*0.207E-01	
3880.33 A	10000.	0.317	0.390E-01	*0.313E-01	*0.234E-01
C= 0.65E+20	20000.	0.246	0.514E-01	0.422E-01	*0.323E-01
	30000.	0.219	0.581E-01	0.472E-01	*0.359E-01
	40000.	0.198	0.634E-01	0.523E-01	*0.398E-01
	60000.	0.174	0.706E-01	0.564E-01	*0.426E-01
(^3P) 4p $^4D^o_{7/2}$ - (^3P) 4d $^4D_{5/2}$	5000.	0.363	0.225E-01	*0.185E-01	
3763.50 A	10000.	0.274	0.350E-01	*0.284E-01	*0.210E-01
C= 0.63E+20	20000.	0.212	0.463E-01	0.378E-01	*0.289E-01
	30000.	0.189	0.521E-01	0.428E-01	*0.323E-01
	40000.	0.170	0.573E-01	0.467E-01	*0.357E-01
	60000.	0.149	0.627E-01	0.501E-01	*0.381E-01
(^3P) 4p $^4D^o_{5/2}$ - (^3P) 4d $^4D_{7/2}$	5000.	0.395	0.242E-01	*0.199E-01	
3844.73 A	10000.	0.301	0.377E-01	*0.305E-01	*0.227E-01
C= 0.67E+20	20000.	0.234	0.498E-01	0.408E-01	*0.312E-01
	30000.	0.207	0.561E-01	0.459E-01	*0.345E-01
	40000.	0.187	0.612E-01	0.504E-01	*0.384E-01
	60000.	0.164	0.683E-01	0.543E-01	*0.410E-01
(^3P) 4p $^4D^o_{3/2}$ - (^3P) 4d $^4D_{5/2}$	5000.	0.391	0.241E-01	*0.199E-01	
3900.36 A	10000.	0.297	0.377E-01	*0.305E-01	*0.226E-01
C= 0.67E+20	20000.	0.230	0.500E-01	0.408E-01	*0.310E-01
	30000.	0.204	0.562E-01	0.461E-01	*0.348E-01
	40000.	0.186	0.617E-01	0.502E-01	*0.383E-01
	60000.	0.162	0.675E-01	0.540E-01	*0.410E-01